Hyperfine Interactions manuscript No.
(will be inserted by the editor)

Mössbauer analysis of Nd-Co M-type strontium hexaferrite powders with different iron content

Carlos Herme · Silvia E. Jacobo · Paula G. Bercoff · Bibiana Arcondo

Received: date / Accepted: date

Abstract The structural analysis of strontium hexaferrites $SrFe_xO_{19}$ (for $x = 12, 11$ and 10) and substituted samples $Sr_{0.7}Nd_{0.3}Fe_{12-y}Co_{0.3}O_{19}$ (for $y = 0.3, 1.3$ and 2.3) prepared through the citrate precursor method is shown. Nd and Co substitution modifies saturation magnetization (M_S) and increases coercivity (H_c) in samples heat-treated at 1100°C for two hours. Mössbauer analyses show different iron occupancy and the influence of the Fe^{3+} content is particularly emphasized. Hematite segregation is observed for some compositions. Samples with low Fe^{3+} content show the best magnetic properties with no secondary phase segregation.

Keywords Strontium hexaferrites · Nd-Co substitution · non-stoichiometric hexaferrite

PACS 75.50.G · 75.60.E · 61.18.F

1 Introduction

The magnetic properties of substituted hexaferrites are strongly dependent upon the electronic configuration of the substituting cations as well as on the Fe^{3+} ions five different intersticial crystallographic sites: three octahedral sites (12k, 2a and 4f2), one tetrahedral site (4f1) and one bipyramidal site (2b). The magnetic structure is ferrimagnetic with different sublattices: three parallel (12k, 2a and 2b) and two antiparallel (4f1 and 4f2) which are coupled by superexchange interactions through the O^{2-} ions [1]. It has recently been shown that the magnetic properties of anisotropic M-type $SrFe_{12}O_{19}$ hexagonal ferrites can be improved by doping with La and Co [2–4]. This improvement is largely related to the coercivity and the magneto-crystalline anisotropy [5]. Wang *et al.* prepared Nd-substituted Sr

C. Herme and S. E. Jacobo
LAFMACEL, Facultad de Ingeniería, UBA, Paseo Colón 850, C1063EHA, Buenos Aires, Argentina.
E-mail: sjacobo@fi.uba.ar

P. G. Bercoff
Facultad de Matemática, Astronomía y Física, Universidad Nacional de Córdoba and IFFAMAF, Conicet. Argentina.

B. Arcondo
Laboratorio de Sólidos Amorfos, Facultad de Ingeniería, UBA, Paseo Colón 850, C1063EHA, Buenos Aires, Argentina.

Table 1 Composition, sample labels and magnetic properties of powders heat-treated at 1100°C for 2 hours.

Sample	Nominal composition	Fe defect	H_c [Oe]	M_{max} [emu/g]	M_S[emu/g]
F12N0	$SrFe_{12}O_{19}$	0	2100	72	91
F11N0	$SrFe_{11}O_{17.5}$	1.0	4930	77	97
F10N0	$SrFe_{10}O_{16}$	2.0	2845	71	89
F12N3	$Sr_{0.7}Nd_{0.3}Fe_{11.7}Co_{0.3}O_{19}$	0.3	4613	60	75
F11N3	$Sr_{0.7}Nd_{0.3}Fe_{10.7}Co_{0.3}O_{17.5}$	1.3	5120	70	87
F10N3	$Sr_{0.7}Nd_{0.3}Fe_{9.7}Co_{0.3}O_{16}$	2.3	4885	64	77

hexaferrite particles hydrotermally synthesised [6]. They reported that saturation magnetization M_S values are almost the same than that of Sr-M whereas their coercivities are around 11% higher. The solubility of rare earth ions in Sr-hexaferrites is very low and their introduction leads to the formation of secondary phases, which must be avoided in order to obtain permanent magnets with optimal properties. Secondary phases such as $SrFeO_3$ and $NdFeO_3$ were observed for all the Sr-rare earth ions substitution. La-Co substituted hexagonal ferrite prepared by the citrate self-combustion route has been tried by different researches [3, 5]. However, complete single-phase formation was not observed for annealing temperatures below 1200 °C.

In this paper we present the novel results for Sr ferrites with Nd-Co substitution. We have recently reported Nd inclusion in strontium hexaferrites [7]. As different iron compounds were reported to be the main secondary phases when rare-earth ions substitution increases [3], we propose a deficient iron formulation. A further improvement of both intrinsic and magnetic properties of the Nd-Co substituted ferrite can be obtained by adjusting the chemical composition. Powders of strontium hexaferrites ($SrFe_xO_{19}$) for $x = 12, 11$ and 10 and substituted samples ($Sr_{0.7}Nd_{0.3}Fe_{12-y}Co_{0.3}O_{19}$ for $y = 0.3, 1.3$ and 2.3) prepared through the citrate precursor method are investigated by Mössbauer spectrometry. The hyperfine parameters deduced from the fittings are discussed in relation with the substitution effects.

2 Experimental

Samples of composition $SrFe_xO_{19}$ (for $x = 12, 11$ and 10) and substituted samples $Sr_{0.7}Nd_{0.3}Fe_{12-y}Co_{0.3}O_{19}$ (for $y = 0.3, 1.3$ and 2.3) were prepared by the self-combustion method. The chemical precursors used for these experiments were $Fe(NO_3)_3 \cdot 9H_2O$, $SrCO_3$, Nd_2O_3, $Co(CH_3COO)_2 \cdot 4\,H_2O$, as it was earlier reported [7,8]. The ratio citric:nitric acid was fixed in 2:1 for each experiment. Aqueous suspensions were stirred and heated for several hours until the sol turned into a dried gel. Then the dried gel was ignited in a corner and a combustion wave spontaneously propagated through the whole gel converting it into loose magnetic powder. Powders were heat-treated in air at 1100°C for two hours. The non-stoichiometric compositions and sample labels for the powders heated at 1100°C are given in Table 1. The oxygen content was calculated assuming the following valences: Sr^{2+}, Nd^{3+}, Co^{2+} and Fe^{3+}.

The structural analysis of the powders was done by x-ray diffraction using a Philips diffractometer and CuK_α radiation. The patterns were taken between 2θ =20° and 70° with a step of 0.02°. A vibrating sample magnetometer Lakeshore 7300 was used to measure the magnetic properties at room temperature. Hysteresis loops *M vs H* were measured with a maximum applied field of 15 kOe. Since the loops did not saturate at 15 kOe, the value of

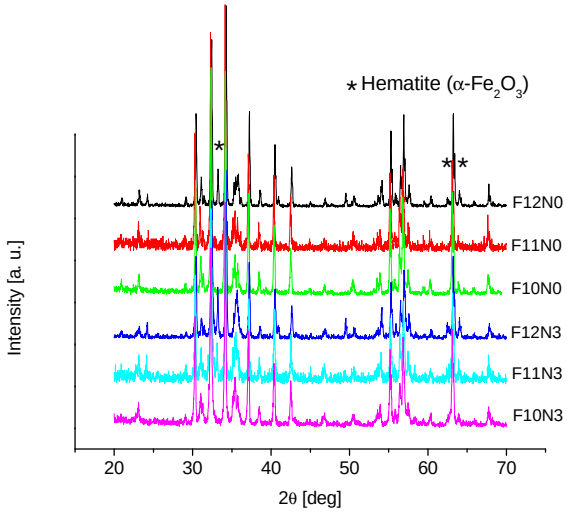

Fig. 1 X-ray diffraction patterns of the studied samples.

saturation magnetization M_S for each sample was calculated by extrapolating M *vs* $1/H$ to 0. Fe Mössbauer spectroscopy (MS) was performed at room temperature, in transmission geometry. ^{57}Co(Rh) source was used with a constant acceleration drive. The spectrometer was calibrated employing an α-Fe foil. Mössbauer spectra were fitted with the NORMOS (SITE) program [9] Isomer shift values are reported relative to $\alpha-$Fe whereas the velocity abscissas of the spectra are relative to the source.

3 Results and discussion

XRD patterns of all the samples are shown in Fig. 1. It is found that they are mainly composed of single-phase magnetoplumbite crystalline structure. Small amounts of hematite are present in samples with higher iron content. In substituted samples neither Nd nor Co compounds were detected indicating that both ions were included in the hexagonal structure. Intermediate phases such as $SrFe_2O_4$ were not observed as it is normally observed in samples synthesized by the ceramic route [10]. This indicates that the solid state reaction is exclusively heterogeneous, and the hexaferrite phase formation proceeds by the formation and growth at the expense of the existing phases – strontium carbonate, hematite and maghemite. This is possible since, in the citrate gel route of synthesis, the mixing of cations takes place at the atomic level, thus reducing the paths of diffusion for various cations, as compared to the ceramic route where the diffusion distances are considerably larger [11]. It may be pointed out that the amount of vacancies at the Fe sites is as high as 16% (for sample F10N0) and yet the hexaferrite structure does not break down nor do any other phases occur indicating that the structure is stable.

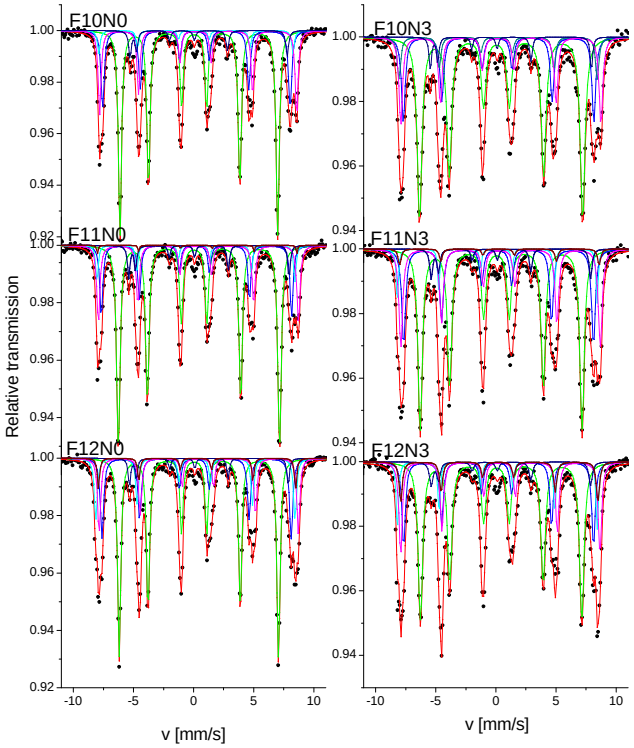

Fig. 2 Room temperature Mössbauer spectra and fittings of $SrFe_xO_{19}$ (left) and of $Sr_{0.7}Nd_{0.3}Fe_{x-0.3}Co_{0.3}O_{19}$ (right) obtained with a $^{57}Co(Rh)$ source.

Table 1 shows magnetic properties of all samples. It can be seen that H_c increases with Nd-Co substitution for all Fe composition (y). These magnetic ions modify superexchange interaction in the magnetoplumbite structure. M_S is slightly modified in all samples since its value depends on composition, crystallinity and the presence of non-magnetic phases as hematite.

Mössbauer spectra of $SrFe_xO_{19}$ (see Fig. 2, left) were fitted with five sextets (one for each crystallographic iron site), except for samples were hematite was detected. In these cases, another contribution for hematite was included. The isomer shifts (δ), that may be attributed to Fe^{3+}, follow the sequence 4f2$\geq$12k$>$2b$>$ 4f1$>$2a whereas the sequence for hyperfine magnetic fields (B_{hf}) is 4f2$\geq$ 2a$>$4f1$>$12k$\geq$2b. Similar results were reported by B. J. Evans *et al.* [12]. However, isomer shift values corresponding to sites 4f1 and 2a are exchanged. This difference may be attributed either to the different synthesis procedure followed in each case or to the intrinsic difficulties found in fitting these complex spectra due to the poorly resolved 4f2, 2a and 4f1 sites contributions. Hyperfine parameters for these samples are reported in Table 2.

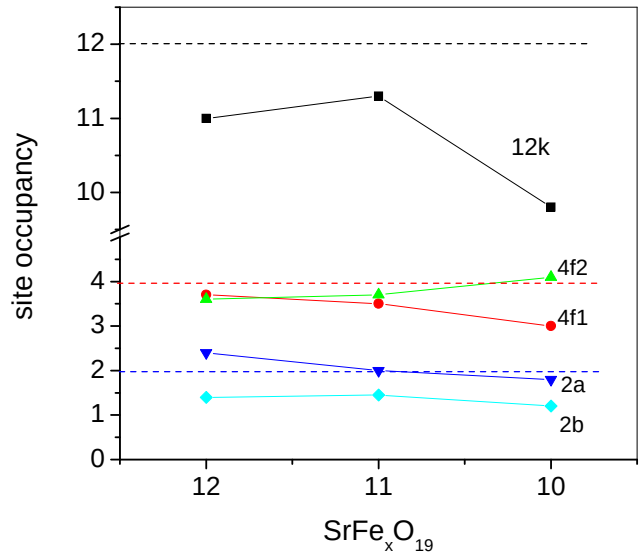

Fig. 3 Fe^{3+} occupancy of the five sites of $SrFe_xO_{19}$ for samples with different iron content (x). Theoretical values for the different sites are indicated by dashed lines.

Fig. 3 shows the site occupancy O_i estimated from Mössbauer results for non-substituted samples with different iron content as $O_i = \frac{N}{A}A_i$, where N is the theoretical number of Fe atoms in the unit cell, A is the total area of the Mössbauer spectrum and A_i is the area of each site contribution. Corrections for hematite presence were considered. Iron vacancies are not proportionally distributed in all sites. The occupancy of sites 12k, 4f1 and 2b is lower than the theoretical values (dashed lines in Fig. 3) and varies with x. From Mössbauer results the effective number of Fe^{3+} spins per cell n = (12k+2a+2b)-(4f1+4f2) for x = 12, 11 and 10 are 7.5, 7.6 and 5.7 respectively, and can be related to M_S (Table 1). The relatively low experimental value of M_S for x=12 (72 emu/g) may be attributed to the presence of hematite (8%) in this sample (F12N0). In our experimental conditions, sample F11N0 shows the best composition for a non-substituted hexaferrite sample as it is monophasic with high M_S and high H_c values (Table 1).

Mössbauer spectra of powders with x= 12, 11 and 10 are shown in Figure 2 (right) and their hyperfine parameters are reported in Table 2. It is observed that B_{hf} and the line width of the 12k contribution increases with substitution, in agreement with an increasing distribution of environments around the 12k site.

The inherent randomness in site occupancy of the different ions and the presence of vacancies (due to non-stoichiometry) appear to be the responsible for the increase in line widths (see Γ in Table 2) whereas the increase in B_{hf} corresponding to 12k sites may be attributed to a perturbation of the superexchange 12k–O^2–4f2 and 12k–O^2–2a interactions due to the presence of Co^{2+} in the 4f2 and 2a sites. Co substitution in 4f2 sites increases B_{hf} on sites 12k due to its magnetic moment, lower than that of Fe^{3+} and opposite to this one. On the other hand, Co substitution in 2a sites decreases B_{hf} on sites 12k due to the common alignment of both magnetic moments. As the number of 4f2 sites in 12k environment dou-

Table 2 Hyperfine parameters for all samples with different iron content. Isomer shift δ, quadrupole splitting Δ and line width Γ are in mm/s, hyperfine field B_{hf} is in Tesla.

Site	Parameter	F12N0	F12N3	F11N0	F11N3	F10N0	F10N3
12k ↑ Octahedral	$\delta(\pm0.01)$	0.35	0.35	0.35	0.35	0.35	0.35
	$\Gamma(\pm0.01)$	0.31	0.45	0.34	0.44	0.32	0.48
	$B_{hf}(\pm0.1)$	41.0	41.6	41.5	41.7	40.6	42.0
	$\Delta(\pm0.01)$	0.39	0.39	0.41	0.39	0.39	0.39
4f1 ↓ Tetrahedral	$\delta(\pm0.02)$	0.27	0.25	0.26	0.25	0.26	0.27
	$\Gamma(\pm0.02)$	0.35	0.35	0.31	0.38	0.32	0.35
	$B_{hf}(\pm0.2)$	48.7	48.9	49.0	48.9	48.3	49.1
	$\Delta(\pm0.01)$	0.19	0.17	0.17	0.17	0.15	0.13
4f2 ↓ Octahedral	$\delta(\pm0.05)$	0.50	0.45	0.40	0.44	0.38	0.41
	$\Gamma(\pm0.02)$	0.30	0.35	0.32	0.38	0.29	0.39
	$B_{hf}(\pm0.2)$	51.3	51.3	51.6	51.4	50.8	51.6
	$\Delta(\pm0.05)$	0.07	0.05	0.22	0.11	0.22	0.22
2a ↑ Octahedral	$\delta(\pm0.03)$	0.24	0.21	0.22	0.19	0.21	0.23
	$\Gamma(\pm0.02)$	0.30	0.35	0.25	0.21	0.27	0.39
	$B_{hf}(\pm0.3)$	51.3	51.5	51.3	51.5	50.1	51.1
	$\Delta(\pm0.01)$	0.04	0.03	0.16	0.05	0.18	0.14
2b ↑ Bi-pyramidal	$\delta(\pm0.01)$	0.27	0.27	0.26	0.27	0.25	0.25
	$\Gamma(\pm0.01)$	0.24	0.37	0.25	0.29	0.27	0.35
	$B_{hf}(\pm0.1)$	40.9	40.9	41.3	41.1	40.5	41.5
	$\Delta(\pm0.01)$	2.21	2.21	2.25	2.18	2.22	2.21

bles that of 2a sites, the net effect is an increase in B_{hf} corresponding to Fe^{3+} in sites 12k. On 4f2 sites δ decreases with Fe defect. This may be attributed to a decrease of Fe–O distance for 4f2 sites due to vacancy in 2b sites. This behavior is accompanied by an increase of the quadrupole splitting Δ. When substitution takes place, δ decreases for site 4f2 in samples with smaller Fe defect. This decrease is attributed to the presence of Nd^{3+} instead of Sr in the vicinity of the 4f2 site in relation with the electron density in the vicinity of this site. Similar results were reported by Lechevallier *et al.* for La^{3+} substitution in hexaferrites [13]. On the other hand, in samples with a larger Fe defect δ increases with substitution. This effect may be attributed to the Co^{2+} for Fe substitution in the neighborhood of sites 4f2, with the consequent effect on electron density on the 4f2 site environment.

In sites 2a, a slight tendency towards the diminution of δ with Fe defect is observed. As for 4f2 sites this effect may be attributed to the decrease of the Fe–O distance due to vacancy of Fe in 12k and 4f1 sites. However, the effect of vacancy in both places is not necessary additive. Hyperfine parameters from 4f1 and 2b sites are not affected neither by Fe defect nor by substitution.

4 Conclusions

Nd-Co substituted hexaferrites were prepared by the self combustion method with different iron content. Magnetic properties enhance with substitution in all samples. Samples F11N3 and F11N0 present the best magnetic properties followed by substituted samples F10N3 and F12N3 even when there is a considerable iron vacancy (near 9%). Mössbauer analysis shows that iron occupancy is related to magnetization values and that hyperfine parameters reflect

the changes that take place in the hexaferrite structure upon Fe defect and substitution of Fe and Sr by Co and Nd, respectively.

Acknowledgements This work was partially supported by CONICET, SeCyT–UNC and UBA.

References

1. J.Smith, H.P.J.Wijn, *Ferrites*, Philips Technical Library, 1959.
2. H. Jonker, H. P. Wijn, P. B. Braun, Phil. Tech. Rev. 18 (1956) 145.
3. F. Kools, A. Morel, R. Grössinger, J. M. Le Breton, P. Tenaud, J. Mag. Mag. Mater. 242-245 (2002) 1270-1276.
4. L. Lechevallier, J. M. Le Breton, A. Morel, P. Tenaud, J. Mag. Mag. Mater. 316 (2007) e109-e111.
5. H. Taguchi, Y. Minachi, K. Masuzawa, Proceedings of the Eighth International Conference on Ferrites, 18-21 September 2000, Kyoto, Japan, 405.
6. J. F. Wang, C. B. Ponton, I. R. Harris, J. Mag. Mag. Mater. 234 (2001) 233-240.
7. S. E. Jacobo, C. Herme and P. G. Bercoff. ”Influence of the iron content on the formation process of substituted Co-Nd strontium hexaferrite prepared by the citrate precursor method”. J. Alloys Compd. (2008) *in press*.
8. N. Rezlezcu, C. Doroftei, E. Rezlezcu, P. D. Popa, J. Alloys Compd. (2007), doi: 10.1016/j.jallcom.2007.04.102.
9. R. A. Brand, Normos Programs, Laboratorium fuer Angewandte Physik, Universitaet Duisburg, 1990.
10. H. How, X. Zuo, C. V. Wave, IEEE Trans. Magn. 41 (2005) 2349.
11. D. Bahadur, W. Fisher, M. V. Rane Mater. Sci. and Eng A 252 (1998) 109-116.
12. B. J. Evans, F. Grandjean, A. P. Lilot, R. H. Vogel, A. Gérard, J. Mag. Mag. Mater. 67 (1987) 123-129.
13. L. Lechevallier, J. M. Le Breton, J.Teillet, A. Morel, F.Kools, P. Tenaud, Physica B 327 (2003) 135-139

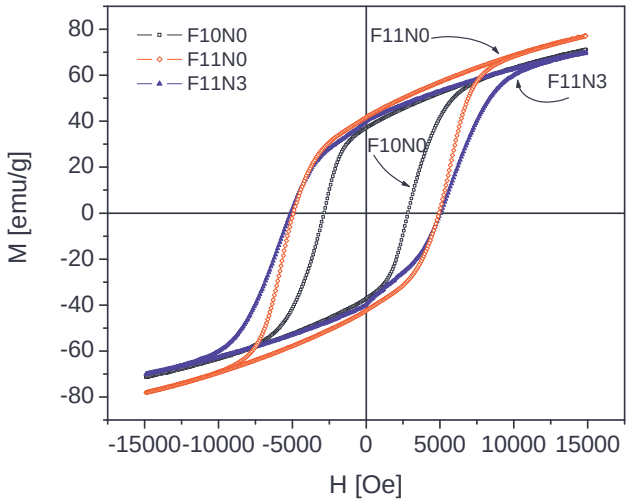

Fig. 4 Hysteresis loops of selected samples.

In case the editors consider it appropriate, this extra figure may be added to the manuscript after Figure 1. If that is so, second paragraph of Section 3 should be changed to:

Table 1 shows magnetic properties of all samples and Fig. 4 shows the hysteresis loops of some of them. It can be seen that H_c increases with Nd-Co substitution for all Fe composition (y). These magnetic ions modify superexchange interaction in the magnetoplumbite structure. M_S is slightly modified in all samples since its value depends on composition, crystallinity and the presence of non-magnetic phases as hematite.